

RSC Advances



This is an *Accepted Manuscript*, which has been through the Royal Society of Chemistry peer review process and has been accepted for publication.

Accepted Manuscripts are published online shortly after acceptance, before technical editing, formatting and proof reading. Using this free service, authors can make their results available to the community, in citable form, before we publish the edited article. This *Accepted Manuscript* will be replaced by the edited, formatted and paginated article as soon as this is available.

You can find more information about *Accepted Manuscripts* in the [Information for Authors](#).

Please note that technical editing may introduce minor changes to the text and/or graphics, which may alter content. The journal's standard [Terms & Conditions](#) and the [Ethical guidelines](#) still apply. In no event shall the Royal Society of Chemistry be held responsible for any errors or omissions in this *Accepted Manuscript* or any consequences arising from the use of any information it contains.

Injectable polysaccharide hybrid hydrogels as scaffolds for burn wound healing

Cite this: DOI: 10.1039/x0xx00000x

Ziyi Li,^a Baoming Yuan,^c Xiaoming Dong,^c Lijie Duan,^{*a} Huayu Tian,^b Chaoliang He,^{*b} Xuesi Chen^b

Received 00th January 2012,
Accepted 00th January 2012

DOI: 10.1039/x0xx00000x

www.rsc.org/

In this study, a type of injectable polysaccharide-based hydrogels were prepared *via* the Schiff-base crosslinking reaction between the amino groups of carboxymethyl chitosan (CMC) and the aldehyde groups of oxidized dextran (Odex). The gelation time of the CMC/Odex hybrid hydrogels was 25 - 50 s, depending on the CMC/Odex weight ratio. The hydrogel displayed a storage modulus of ~1 kPa, and the freeze-dried hydrogel showed an interconnected porous structure. The *in vitro* degradation test of the hydrogel in PBS showed a fast mass loss in the first 2 days, and then a gradual degradation profile over 4 weeks. The *in vitro* cytotoxicity and the ability to support cell attachment of the hydrogels were tested by incubation with L929 cells. The results indicated that the hydrogels displayed good cytocompatibility, and the hydrogels with relatively higher CMC content supported the attachment of L929 cells. Moreover, the potential application of the hydrogels in burn wound healing was tested on SD rats with a deep second-degree burn wound. It was found that the group treated with the CMC/Odex hydrogel showed nearly complete wound closure at 21 days after the treatment compared to unsatisfactory wound healing efficiency of the untreated group. Additionally, the histological analysis by H&E and Masson's trichrome staining indicated clearly the regeneration of skin appendages, including hair follicles, sebaceous glands and dermal papillary, suggesting that the treatment with the hydrogel promoted the wound healing and skin regeneration. Overall, the injectable polysaccharide hybrid hydrogels may serve as suitable scaffolds for promoting burn wound healing and skin regeneration.

Introduction

Burn injuries are among the most serious injuries and cause more severe physiological stress than other traumas.^{1,2} Compared with incisional or excisional wound, the healing mechanism of burn wounds is very different.^{3,4} After burn injuries, the necrotic eschar tissue impedes early wound closure and could expand into deeper tissues. Tissue regeneration is hampered by the progressive necrosis and the initiation of inflammatory response, leading to the delay of wound reepithelialization.⁵⁻⁸ Recently, burn treatments have attracted considerable attention due to approximately a million patients suffering burns, an estimated 40,000 hospitalizations and 3400 deaths annually according to the American Burn Association.⁹

Many methods have been developed for burn wound healing. In clinical practice, the patients are treated by transplanting tissue from the same body to the defective sites. Although the surgery is a useful strategy for considerable lives, the patient may suffer side-effects such as permanent use of immunosuppressive agents, viral infection, donor site morbidity and secondary surgery.¹⁰ Moreover, scar-like dermal structures and shrinkage will emerge because of the deficiency of nutrients,

growth factors, and oxygen during the process.¹¹ In the past few years, a tissue-engineered dermal-epidermal skin substitute (DESS)¹² have been used as the current clinical gold-standard to save countless lives; however, it also has many limitations such as donor-site shortage, propensity to contraction, shrinkage and scarring.^{13,14}

To overcome these shortcomings, hydrogel-based scaffolds have been proposed as an alternative to treat burns.¹⁵⁻¹⁹ The regeneration of skin is difficult after a large area of burn without the aid of a scaffold. Hydrogels have the ability to form *in situ* from free flowing polymer solution to gel in burn skin by physical or chemical means.²⁰⁻²⁵ Thus, the scaffolds and the burn sites could closely contact to offer an ideal hydration environment. Additionally, hydrogels are structurally similar to the natural extracellular matrix,²⁶ facilitating the gaseous and nutrient exchange to the wound bed. Moreover, hydrogels are able to absorb the exuding liquids and debris and further maintain the wound surface moist, which is significant for cell migration and skin regeneration.

Naturally derived materials are promising biomedical materials due to their advantages such as similarities to the

extracellular matrix, good biocompatibility and inherent cellular interaction.²⁷ Among them, chitosan is known to promote drainage, prevent the building up of exudates, and promotes gas exchange, which are essential in wound healing process. Negative charge on skin surface enables electrostatic binding of chitosan (cationic polymer) to the skin surface.²⁸ Moreover, chitosan has known potential in treatment of burns because of its intrinsic antimicrobial properties.²⁹ In addition, dextran has been extensively investigated for their potential in biomedical applications, such as in scaffolds for tissue engineering and carriers for delivery of drugs or proteins, owing to its good biocompatibility and anti-fouling properties as well as the feasibility of modification via the hydroxyl side groups.³⁰ An ideal wound scaffold should protect the wound from bacterial infection, control evaporative water loss and prevent dehydration, allow diffusion of oxygen and carbon dioxide, absorb wound exudate, and promote healing.³¹

In this study, injectable chitosan/dextran hybrid hydrogels were prepared through the *in situ* formation of Schiff-base linkages between chitosan and dextran derivatives. The physicochemical properties, including gelation time, degradation period, and mechanical property, were characterized. The *in vitro* cytotoxicity of the hydrogels was evaluated by incubation of L929 cells with the eluent of the hybrid hydrogels formed at various chitosan/dextran ratios. The influence of chitosan content on the cell adhesion was studied, since the adhesive chitosan may keep the migrated cells retain on the defect site.³² Finally, the potential of the polysaccharide hybrid hydrogels in burn treatments was evaluated *in vivo* by using a burn wound model on SD rats.^{26, 33}

Experimental

Materials

Chitosan (low molecular weight) and dextran (Mw = 100KDa) were purchased from Sigma-Aldrich (USA) and used without further purification. Chloroacetic acid and sodium periodate (NaIO₄) were provided by Alladin (China). 3-(4,5-dimethyl-thiazol-2-yl)-2,5-diphenyl tetrazolium bromide (MTT) was obtained from Sigma-Aldrich (USA). All the other reagents were used as received.

Synthesis of oxidized dextran and carboxymethyl chitosan

Oxidized dextran (Odex) was successfully synthesized by methods as reported previously.³⁴ Briefly, 2.00 g of dextran was dissolved into 50 mL of sodium dihydrogen phosphate buffer solution (1/15 M). Then, 0.44 g of NaIO₄ was added into the reaction liquid. The mixture was stirred at room temperature for 2h, followed by a 3 day dialysis in distilled water and lyophilization to obtain the final product. The degree of oxidation was determined by hydroxylamine hydrochloride method.³⁵

Carboxymethyl chitosan (CMC) was prepared according to the previous method.³⁶ Chitosan (10.00 g) and sodium hydroxide (13.50 g) were swelled and alkalinized into 100 mL of

isopropanol/water (50/50, v/v) solution with continuous stirring at 50 °C for 2 h. Then, 2.94 g of monochloroacetic acid (dissolved in 20 mL of isopropanol) was added into the reaction mixture dropwise and reacted for 4 h at the same temperature. After that, 200 mL of 80% ethyl alcohol was added to stop the reaction, followed by filtering to obtain the solid sodium salt. The solid was rinsed in 80% ethyl alcohol to desalt and dewater, and dried under vacuum at room temperature. Then, 37% hydrochloric acid (10 mL) was added into the solid sodium salt (suspension in 80% ethyl alcohol), the mixture was stirred at room temperature for 30 min. Then, the solid was filtered and rinsed in 80% ethyl alcohol, followed by vacuum drying.

Preparation of carboxymethyl chitosan/oxidized dextran hybrid hydrogels

Oxidized dextran and O-carboxymethyl chitosan were dissolved into phosphate buffer solution (PBS, 0.01M, pH = 7.4) to form 3% (w/v) solutions, respectively. To investigate the effect of contents of oxidized dextran and O-carboxymethyl chitosan on the properties of hydrogels, a 3% oxidized dextran solution was mixed with a 3% carboxymethyl chitosan solution at various volume ratios (1:2, 1:1, 2:1). The resulting mixed solutions were kept at room temperature to obtain the cross-linked hydrogels, and the gelation times were recorded. The formation of hydrogels was determined by the test tube inverting method, when the mixture could not flow within 30s after the test tube was inverted.

Degradation behavior

Hydrogel samples (0.8 mL) were prepared in vials (diameter = 16 mm) by the method described above. The initial masses of the vials and the vials including the hydrogels were accurately weighed (W₀). Subsequently, 3 mL of PBS (0.01M, pH 7.4) was added gently and the vials were incubated at 37 °C. The PBS solution were removed carefully from the surface of the hydrogel at different time intervals, and the samples were weighed to obtain the masses of the remaining hydrogels (W_t). The experiments were performed in triplicate. The degree of the *in vitro* degradation was calculated by the following equation:

$$\text{weight remaining (\%)} = W_t / W_0 \times 100\%$$

Rheological experiments

Rheological measurements were carried out with a MCR 301 Rheometer (Anton Paar) with parallel plates of 25 mm diameter at a constant temperature of 37 °C. The gap between the plates was set at 0.5 mm. The 3% CMC and Odex solutions were mixed in at a volume ratio of 2:1 using an oscillator, and the mixture was placed immediately on the plate of the rheometer. A layer of silicon oil was placed around the samples to prevent the evaporation of water. Storage moduli (G') and loss moduli (G'') were monitored as a function of time at a frequency of 1 Hz and a strain of 1%.

Morphology of hydrogels

To observe the morphology of the hydrogel, 3% (w/v) of oxidized dextran solution and 3% O-carboxymethyl chitosan solution were mixed (v:v = 1:2) to allow the formation of hydrogel. Then, the sample was snap frozen in liquid nitrogen and subsequently lyophilized for 3 days. The dried sample was coated with gold and measured by scanning electron microscope (Micrion FEI PHILIPS).

***In vitro* cytocompatibility**

The cytotoxicities of the CMC/Odex hybrid hydrogels were evaluated using MTT assay. A mouse fibroblast cell line (L929), which stands for a typical dermal cell, was used for the *in vitro* cytocompatibility test. The hydrogel extract was prepared by incubation the hydrogel with PBS (pH=7.4) for 24 h at 37 °C. The L929 cells were seeded in 96-well plates at a density of 1×10^4 per well followed by incubation in 100 μ L of DMEM at 37 °C under 5% CO₂ for 24 h. Then, the media was replaced with fresh culture medium. The leachates were double-diluted and added into the 96-well plates. Subsequently, the cells were incubated for 24h before adding 20 μ L of MTT (5mg/mL) in each well. After that, the cells were incubated at 37 °C for another 4 h and then precipitated formazan was dissolved in 150 μ L of DMSO. The viability ratio (%) was estimated by measuring the absorbance value at 490 nm on a microplate reader (ELx 680, BioTek Instrument Inc, USA), and calculating according to the following formula:

$$\text{viability (\%)} = (A_{\text{sample}}/A_{\text{control}}) \times 100\%,$$

where A_{sample} and A_{control} are the absorptions at 490 nm for the experimental and control wells, respectively.

***In vitro* cell viability and attachment study**

The cell viability was further estimated by a live-dead cell staining kit. Briefly, 0.3 mL of CMC/Odex hydrogels were prepared in 24-well plates at different CMC/Odex ratios (2:1, 1:1, 1:2) and incubated for 20 min at 37 °C. Then, 1 mL of DMEM containing L929 cells (5×10^4 cells/well) were added to the surface of the hydrogels at 37 °C and incubated for 24 h. After 24 h of incubation, the media was discarded and 0.5 mL of PBS containing 1 μ M calcein AM and 1.5 μ M propidium iodine (PI) was added to each well, followed by indicating for another 30 min. Subsequently, the cells were observed by a fluorescent microscope and images of the cells were captured using CCD.

To further perform cell attachment study, L929 cells were seeded onto a clean coverslip in 6-well culture plates at a density of 5×10^4 cells/well and cultured for 24 h in 2 mL of complete Dulbecco's modified Eagle's medium (DMEM) containing 10% fetal bovine serum, supplemented with 50 IU/mL penicillin and 50 IU/mL streptomycin. Then, the supernatant was carefully removed and the cells were washed thrice with PBS. Subsequently, the cells were fixed with 1.0 mL of 4% formaldehyde for 15min, permeabilized with 0.1% Triton X-100 for 10 min and washed four times with PBS respectively. After that, the cell nucleus were stained with 4,6-diamidino-2-phenylindole (DAPI) and Alexa Fluor488

phalloidin was applied for F-actin. After the samples were mounted and sealed, CLSM images of cells were obtained through confocal microscope (Olympus FluoView 1000).

Animal Procedure

Experimental procedures performed in this study were approved by the policies of Jilin University School of Medicine. 16 male SD rats weighing 200 ~ 250 g were anesthetized by intraperitoneal injection of chloral hydrate (30.0 mg kg⁻¹) and the hair on their upper back was shaved. Subsequently, the surgery area of animals was heated with a stainless steel rod (1 cm diameter) heated to 100 °C. To obtain a severe burn wound model, burn wound excisions were performed after 48 h. Briefly, the resulting dead area was removed surgically by following current clinical practice. Then, the rats were divided into 2 groups randomly as follows: the treated group (n=8) were covered with CMC/Odex hydrogels and the control group (n=8) were only covered with elastic bandage. Additionally, the dressings were renewed every other day and the picture of the burn wounds were collected on day 2, 7, 14, and 21 with a digital camera.

Histological analysis

Tissue samples were collected and fixed in 4% (W/V) PBS-buffered paraformaldehyde. After fixation, samples were embedded in paraffin following by cutting into 3 mm frozen sections with a cryostat microtome. After the samples were stained with H&E and Masson's trichrome, all images were recorded by a light microscope.

Statistic Analysis

SPSS (Version 13.0, Chicago, IL, USA) was used to analysis statistical significance. Significant difference was reported if the p value was less than 0.05. All data were presented as means \pm standard deviations.

Results and discussion

Synthesis of CMC and Odex

The oxidized dextran was prepared through specifically oxidized cleavage of the vicinal glycols in dextran by periodate to form aldehyde groups that could serve as a macromolecular cross-linker with good biocompatibility.³⁴ Furthermore, the degree of oxidation of dextran was determined to be 20% based on hydroxylamine hydrochloride method.

Chitosan and its derivatives have shown potential in wound-healing applications, due to their excellent biocompatibility, biodegradability, and antimicrobial activity.^{37,38} However, chitosan is insoluble in aqueous solution at neutral pH, which limits its biomedical applications. To improve its water solubility, carboxymethylation of chitosan is an efficient method.^{39,40} In this study, chloroacetic acid is used to introduce carboxymethyl groups onto chitosan. After the carboxymethyl groups were incorporated into chitosan, the solubility of the derivative at neutral pH was markedly improved, which facilitates the practical applications of the material.

Preparation and characterization of CMC/Odex hydrogels

The Odex and CMC aqueous solutions were simply mixed to form transparent hydrogels. After mixing the Odex and CMC solutions, the transparent mixed solutions underwent a rapid sol-gel transition at physiological temperature, as shown in Figure. 1. The polysaccharide-based mixtures transformed into a gel state without the necessary of adding any additional crosslinking agent, indicating

good biocompatibility during the gel formation process. Moreover, it is noteworthy that the transparency of the hydrogels benefits for wound observation compared other opaque wound dressing.⁴¹ The mechanism of gelation was schematically illustrated in Figure. 1. Briefly, the aldehyde groups in Odex were reacted with the amino groups in CMC to form the Schiff base linkages at physiological conditions, resulting in the formation of intermolecular crosslinking.⁴²

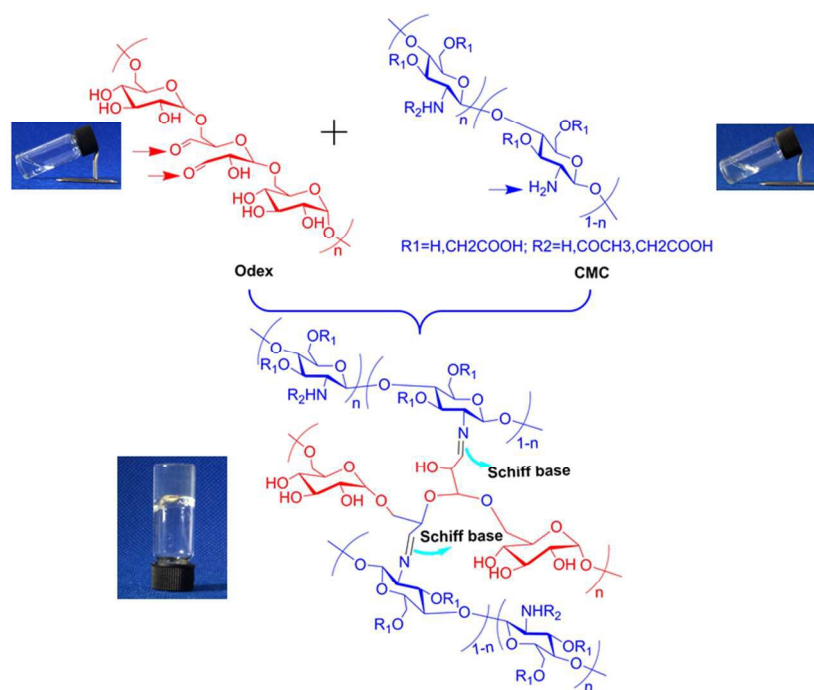


Fig. 1. The formation of CMC/Odex hybrid hydrogel based on Schiff-based reaction. Images of transparent hydrogels obtained by simply mixing the 3 wt% Odex and CMC aqueous solutions.

The gelation time of CMC/Odex hydrogels was also monitored at room temperature. To further evaluate the effect of the feed ratio of CMC to Odex on the gelation time of hydrogels, a 3wt % CMC aqueous solution was mixed with a 3% Odex aqueous solution at various volume ratios (1:2, 1:1, and 2:1). As presented in Fig. 2, gelation occurred within 25 - 50 s following mixing the solutions. With decreasing the CMC/Odex ratio from 2.0 to 0.5, the gelation time reduced from ~ 52 s to 25 s. It can be explained that the gelation time of the hydrogels depends on the ratio of the aldehyde groups of Odex to the amino groups of CMC. Therefore, in this study, the reduction in the gelation time with the increase in the Odex content was likely due to the increase in the crosslinks in the composite hydrogels.⁴² It is noteworthy that an appropriate gelation time plays an important role in practical applications. In the present system, the hybrid hydrogel with the CMC/Odex ratio of 2.0 displayed a gelation time (~ 50 s) suitable for burn wound treatments, which may ensure the close contact between the hydrogels and the burn sites.

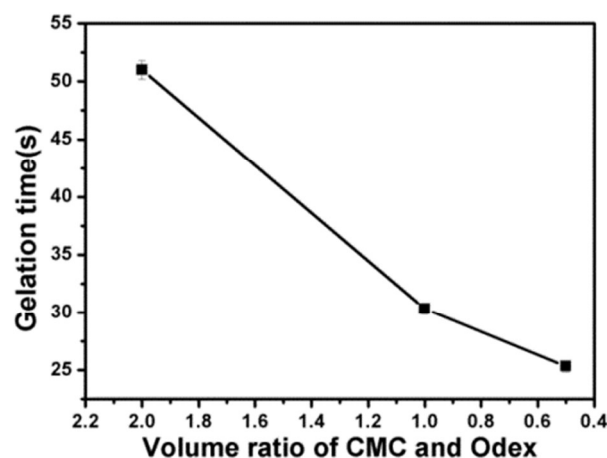


Fig. 2. Gelation time of CMC/Odex hydrogels with different CMC/Odex ratios.

Furthermore, the viscoelastic property and the gelation process of the CMC/Odex hydrogel was investigated by monitoring the variation of the storage modulus (G') and loss modulus (G'') as a function of time during the crosslinking process. The storage modulus (G') serves as an indicator of the stiffness of a viscoelastic material while the G'' stands for viscous loss modulus.²⁵ As shown in Fig. 3, the G' elevated rapidly in the initial stage when compared with G'' , due to the gradual formation of elastic hydrogel resulted from the crosslinking network of Schiff base. Moreover, the G' was significantly higher than G'' , which implied that solid-like behavior dominates the viscoelastic properties of the hydrogel.⁴² As the gelation proceeded, the network was strengthened gradually caused by the Schiff-base reaction between the aldehyde residues of Odex and amino residues of CMC. It suggested that the Schiff-base reaction was almost completed when the G' reached a plateau of ~ 1 KPa.

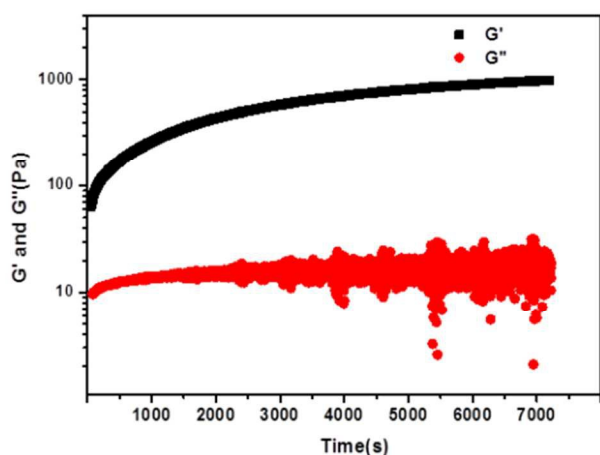


Fig. 3. Storage and loss moduli of the CMC/Odex hydrogel as function of time following mixing the CMC and Odex solutions (CMC/Odex = 2:1 (w/w)).

In vitro degradation was performed by incubating the hydrogels in a 0.01M PBS at 37 °C, and the weight loss of the hydrogels was examined. In the initial period, a small fraction of uncrosslinked or less-crosslinked components hydrolyzed and diffused rapidly from the hydrogel, leading to the fast 20% mass loss of the hydrogels in the first 2 days. Subsequently, the hydrogels underwent a relatively slower degradation process. About 50% of the hydrogels were degraded in 4 weeks (Fig. 4). This might be due to gradual hydrolysis of the Schiff base linkages of the hydrogel with a higher extent of crosslinking.

Besides, the morphology of the freeze-dried CMC/Odex hydrogel was observed by SEM. As shown in Fig. 5, the hydrogels indicated a porous structure. It should be mentioned that keeping moisture at the wound surface is a critical principle for burn treatment. The porous structure may benefit the preservation of moisture at the wound site. Furthermore, the porous structure may facilitate the permeation of bioactive molecules and exudate absorption. Consequently, the

advantages mentioned above may have positive effects on the burn wound repair.

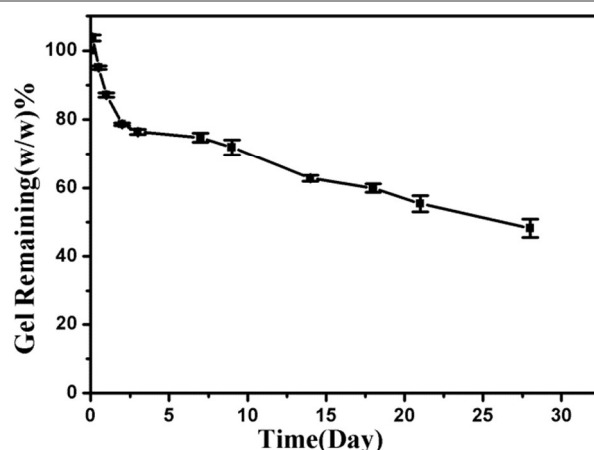


Fig. 4. *In vitro* mass loss profiles for the 3 wt% CMC/Odex hydrogels (CMC/Odex = 2:1 (w/w)) after incubation in PBS (pH 7.4) at 37 °C.

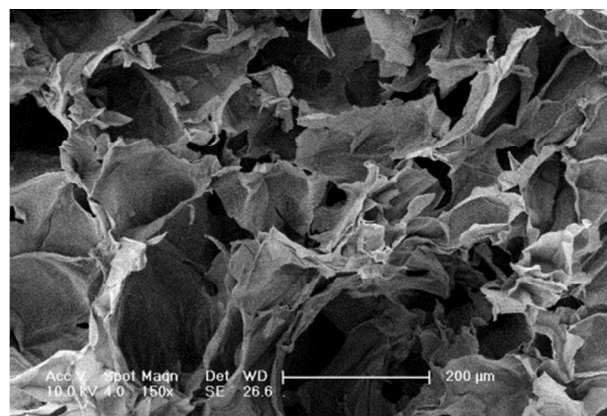


Fig. 5. SEM image for the freeze-dried sample of 3 wt% CMC/Odex hydrogel (CMC/Odex = 2:1 (w/w)).

In vitro viability and adhesion study

The *in vitro* viability of the 3 wt% CMC/Odex (weight ratios = 2:1, 1:1, 1:2) hydrogels was assessed by MTT assay against L929 mouse fibroblasts. The L929 cells were incubated with the double-diluted leachates for 24 h. The cell viabilities were over 85% at all concentrations of the hydrogel extracts (Fig. 6), suggesting no obvious cytotoxicity of the hydrogels. The good cytocompatibility of the hybrid hydrogels should be related to the biocompatible components based on the polysaccharide derivatives.⁴³ Additionally, the hydrogels were formed via a mild, biocompatible Schiff-base reaction without introducing cytotoxic groups into the gels. Therefore, the good cytocompatibility of the CMC/Odex hybrid hydrogels may create a biocompatible microenvironment for cell survival, making them interesting for *in vivo* applications.⁴⁴

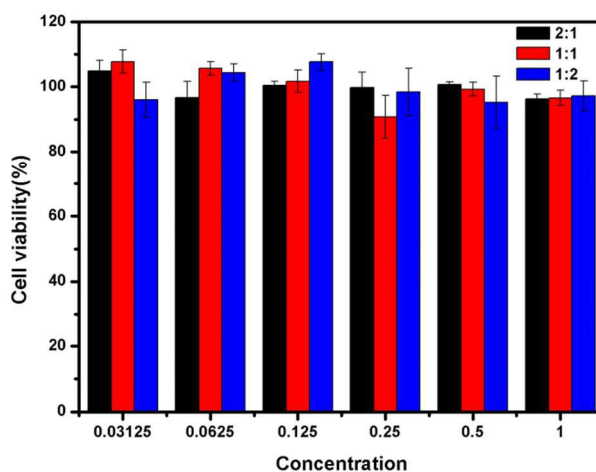


Fig. 6. Viabilities of L929 cells after exposure to the eluants of the 3 wt% CMC/Odex hydrogels (weight ratio = 2:1, 1:1, 1:2) for 24 h as measured *via* MTT assay (n=3): The initial eluent were taken as 1, other concentrations were obtained by double dilution method.

To further investigate cell viability *in vitro*, the L929 cells were seeded on the surface of the hydrogels and cultured for 24h, followed by double stained with AM/PI in the live-dead cell staining experiment. The live cells were stained green while the dead ones were stained red. It was found that most of L929 cells on the surface of the polysaccharide hybrid hydrogels were stained green with calcein-AM (Fig. 7A), suggesting a high viability of L929 cells on the surface of the hydrogels. Although no significant difference in cell viability, L929 cells on the surface of 3wt%CMC/Odex (ratios 2:1) hydrogels seemed to exhibit well-spread morphology when compared with the cells on the surface of 3wt%CMC/Odex (ratios 1:1, 1:2) hydrogels (Fig. 7A). Therefore, we have performed further cell attachment experiments using L929 cells to verify whether the cells attachment on the surface of the hydrogels. L929 cells were seeded on the surface of polysaccharide hybrid hydrogels and incubated for 24h. The cells were treated with Alexa Fluor488 phalloidin and 6-diamino-2-phenylindole dihydrochloride (DAPI, Sigma) to stain for F-actin and nuclei, respectively. As presented in Fig.

7B, the cells on the surface of the 3wt% CMC/Odex with relatively lower carboxymethyl chitosan contents (CMC/Odex = 1:1, 1:2) were retained round in shape, suggesting a poorly-spread morphology. In contrast, a better adhesion morphology of the cells was observed on the hydrogel with the CMC/Odex ratio of 2:1 after 24 h of incubation. The results indicated that the hydrogel with the CMC/Odex ratio of 2:1 could support the attachment of L929 fibroblast. It was pointed out that the materials used for burn wound healing should have the abilities of guaranteeing uniform cell distribution and maintaining cell viability and phenotype,^{45,46} as well as inducing the migration and proliferation of epithelial cells, fibroblasts, and endothelial cells.⁴⁷ Since the CMC/Odex (2/1) hydrogel showed good cytocompatibility and promote the cell attachment *in vitro*, the polysaccharide hydrogels may have potential applications for burn wound healing.

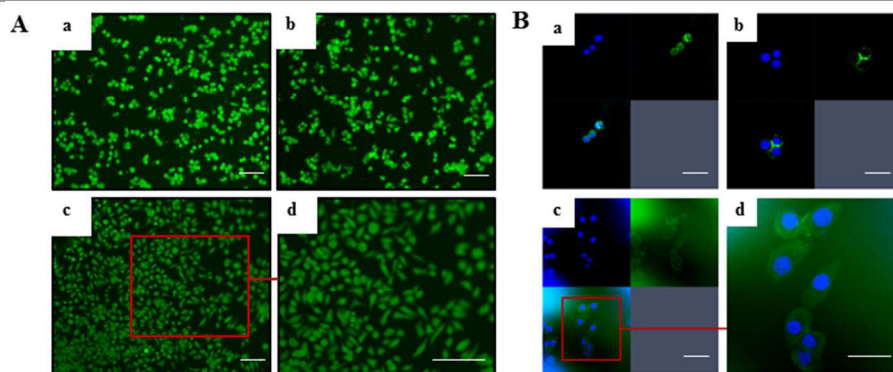


Fig. 7. (A) *In vitro* L929 cells viability on the surface of the 3 wt% CMC/Odex hydrogels. Cells were stained with calcein-AM and PI. Live and dead cells show green and red fluorescence, respectively. The weight ratios of CMC/Odex were 1:2 (a), 1:1 (b), 2:1 (c), respectively. Enlarged image (d). Scale bars indicate 200 μm . (B) *In vitro* L929 cells attachment on the surface of the 3 wt% CMC/Odex hydrogels. Cell nuclei stained with DAPI (blue), F-actin stained with Alexa Fluor 488 phalloidin (green). The weight ratios of CMC/Odex were 1:2 (a), 1:1 (b), 2:1 (c), respectively. Enlarged image (d). Scale bars indicate 50 μm .

Macroscopic evaluations of burn

The potential application of the CMC/Odex hydrogel (3 wt%, CMC/Odex = 2:1 (w/w)) for burn treatments was evaluated on SD rats model with a deep second-degree burn wound. The procedure of the treatment was illustrated in Fig. 8A. Briefly, the relatively small scar was created and burn wound excision was performed after 48 h following current clinical practice. Then, the rats were divided into 2 groups randomly, including the treated and control groups ($n = 8$). The wound sites of the treated group were closely covered with the same size of hydrogel formed *in situ*. In our procedure, the hydrogels were administrated to the wound sites through simple injection. Moreover, our procedure ensures the hydrogel intact and in place for the entire healing period.

Then, the burn wound tissues served as pathological sections were further evaluated by H&E staining to confirm the burn degree. As shown in Fig. 8B, it was found that the dermal-epidermal junction disappeared and skin appendages were basically damaged after the burn, suggesting the generation of deep second-degree burn wounds.

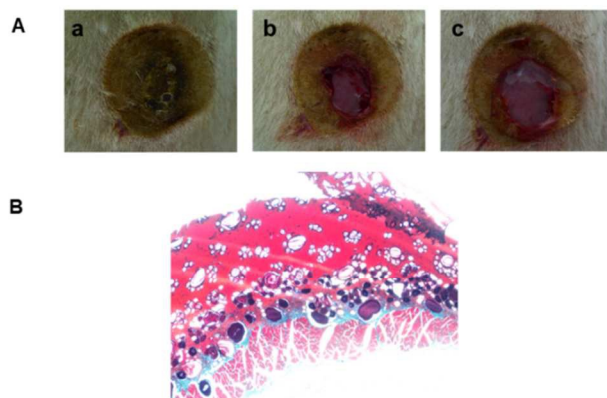


Fig. 8. (A) The procedure of the treatment for deep second burn wound. (B) H&E staining on eschar to analysis the burn degree.

The healing progress was monitored at different time points along the 3 weeks after the treatment. The healing rate of wound closure is an important indicator to evaluate the effect of treatment because the skin acts as a major barrier function in protecting the host against pathogens. Once the skin barrier is damaged, the immune system would produce cytokines to repel invading pathogens. However, excessive inflammation would occur followed by the overproduction of cytokines (a cytokine storm) in severe burn injuries, which can trigger organ failure and cause patient mortality.⁴⁸ By accelerating the rate of wound closure and restoring the skin barrier, the risk of prolonged inflammation is dampened. Therefore, we evaluated the rate of wound closure by macroscopic observations, as shown in Fig. 9. On day 7 following treatment, it was clearly observed the formation of the burn scars in both groups. On day 14, it is noticeable that the wound contraction in the treated group occurred faster than in the control group. Moreover, it was observed that red and swollen phenomenon appears in the burn sites of the untreated group, likely caused by the inflammatory response. Notably, the wounds treated with the hydrogels showed nearly complete healing at 21 days after the treatment, whereas the wound healing was not ideal in the untreated group. This suggested a superior wound healing efficiency of the groups treated with the hydrogel.

In general, wound repair has three classic stages: (i) inflammation; (ii) proliferation, including granulation tissue formation; and (iii) matrix formation and remodelling. The cell attachment test *in vitro* indicated that the chitosan derivative has the ability to promote cell attachment; therefore, the significant effect on the formation of wound granulation tissue may suggest that the hydrogels facilitated epithelial cell migration or homing to the wound area and supported epithelial

differentiation. As a result, it further promoted the skin regeneration followed by matrix formation and remodelling. Besides, it has been established that the risk of scar formation could be reduced if burns primarily heal in less than 21 d. Otherwise, unsatisfactory scars would form if healing remains

incomplete within 21 d.⁴⁹ In this study, skin regeneration was observed in the treated group on day 21, suggesting the the CMC/Odex hydrogel have potential in accelerating the healing of burn wounds within a specific period of time.



Fig. 9. Macroscopic evaluations of the healing of deep second burn wounds with or without the treatment by hydrogel at different time intervals. Scale bars represent 0.25 cm.

Histological examination on healing burns

Histological analysis was performed by H&E and Masson's trichrome staining to further evaluate the process of burn healing at time intervals within 3 weeks (Fig. 10 and 11). As shown in Fig. 10, for the untreated wounds, fibrous tissue was disordered in the early stage (on day 7). Moreover, hair follicles and sebaceous glands were not observed though the fiber structure became normal in untreated wounds within 21 days. In contrast, a gradual improvement in wound healing was clearly observed after application of the hydrogel. The new hair follicles and sebaceous glands existed while the fiber structure was still disordered after 2 weeks of treatment. In addition, the structural integrity of the skin was observed including mature epithelial morphology with hair follicles and sebaceous glands at 21 days following treatment. It was reported by Ito et al. that nascent follicles arise from epithelial cells outside of the hair follicle stem cell niche, suggesting that epidermal cells in the wound assume a hair follicle stem cell phenotype.⁵⁰ Thus, the

formation of hair follicles in the treated group suggests that the hydrogel have a critical influence on the proliferation and differentiation of epithelial cells, which is in accordance with the results of cell attachment above. Additionally, the hydrogels served as burn wound dressings play an important role in maintaining moist environment and inducing autolytic debridement of the necrotic eschar tissue. Autolytic debridement is preferred over physical methods to remove the necrotic eschar, which also benefits the wound healing.⁵¹ Meanwhile, to further analysis therapeutic efficacy of CMC/Odex hydrogels, the tissues of the treated group were further analyzed by Masson's trichrome staining. Fig. 11 shows no obvious collagen structures were observed at 7 days after the treatment. However, it is clearly observed that skin appendages formed in dermal layer and collagen structures showed more organized arrangement at 21 days. Therefore, the results of histological analysis clearly indicated that the polysaccharide-based hydrogels can promote skin regeneration.

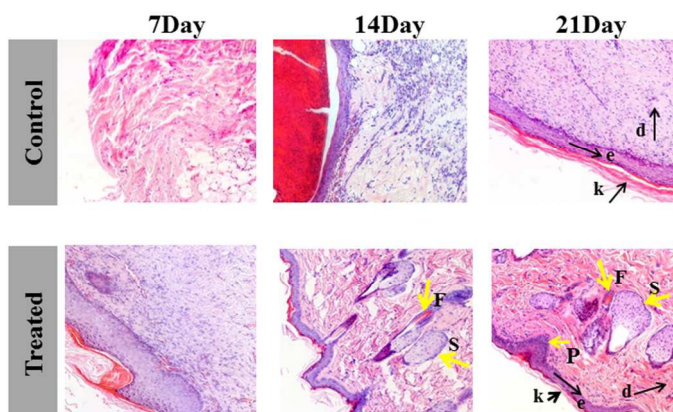


Fig. 10. H&E-stained histologic sections of burn wounds at various time intervals within 3 weeks. Control group: without treatment; Treated group: treated with 3 wt% CMC/Odex hydrogels (CMC/Odex = 2:1 (w/w)). Abbreviations: p, dermal papillae; E, eschar; F, follicle; S, sebaceous gland; k, keratinized layer; e, epidermis layer; d, dermis.

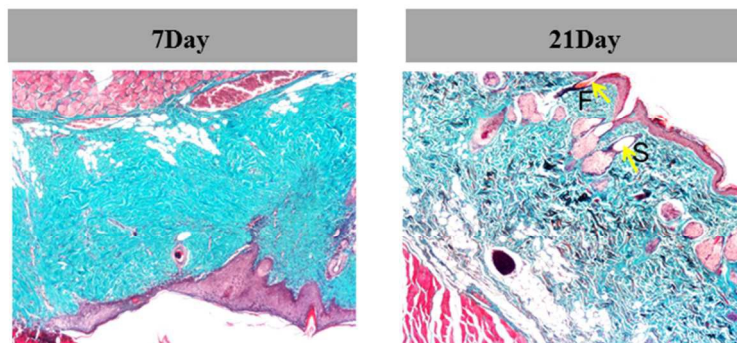


Fig. 11. Masson's trichrome stained histologic sections of the treated burn wounds. F, follicle; S, sebaceous gland.

Conclusion

In this study, an injectable CMC/Odex hybrid hydrogel was prepared through the Schiff-base reaction between the amino groups of CMC and the aldehyde groups of Odex. The gelation time was affected by the CMC/Odex weight ratio. The degradation of the hybrid hydrogel *in vitro* displayed a fast mass loss in the first 2 days followed by a gradual degradation profile over 4 weeks. SEM observation indicated an interconnected porous microstructure of the hydrogel. *In vitro* incubation of the leachates with L929 cells suggested a good cytocompatibility of the hydrogel, and the hydrogel with the CMC/Odex weight ratio of 2 could support the attachment of L929 cell on the surface of the hydrogel. Furthermore, the potential of the hybrid hydrogel in promoting burn wound healing was evaluated by a rat model with a deep second-degree burn wound. The wounds treated with the hydrogels

Not Notes and references

^a School of chemistry and life science, Changchun University of Technology, Changchun 130012, P.R. China. E-mail: duanlijie@ciac.ac.cn

^b Key Laboratory of Polymer Ecomaterials, Changchun Institute of Applied Chemistry, Chinese Academy of Sciences, Changchun 130022, P.R. China. Tel/Fax: +86 431 85262116. E-mail: clhe@ciac.ac.cn

^c Department of Orthopaedics, The Second Hospital of Jilin University, Changchun 130041, P.R. China.

1. S. Sen, D. Greenhalgh and T. Palmieri, *J Burn Care Res*, 2009, **31**, 836–848.
2. P. J. Fagenholz, R. L. Sheridan, N. S. Harris, A. J. Pelletier and C. A. Camargo, *J Burn Care Res*, 2007, **28**, 681–690.
3. S. Monstrey, H. Hoeksema, J. Verbelen, A. Pirayesh and P. Blondeel, *Burns*, 2008, **34**, 761–769.
4. K. M. Merz, M. Pfau, G. Blumenstock, M. Tenenhaus, H. E. Schaller and H. O. Rennekampff, *Burns*, 2010, **36**, 477–482.

exhibited nearly complete healing at 21 days after the treatment, compared to not ideal healing efficiency of the untreated group. In addition, the H&E and Masson's trichrome staining confirmed that the hydrogels accelerated the regeneration of skin with skin appendages, including hair follicles, sebaceous glands and dermal papillary. Therefore, the polysaccharide-based hydrogels may hold potential as scaffolds for promoting burn wound healing and skin regeneration.

Acknowledgements

The authors are grateful for the financial support from the National Natural Science Foundation of China (projects 21574127, 51233004, 51390484 and 51321062), the Ministry of Science and Technology of China (International cooperation and communication program 2011DFR51090), and Jilin province science and technology development program (20130206058GX, 20130521011JH).

5. L. Cuttle, M. Kempf, G. E. Phillips, J. Mill, M. T. Hayes, J. F. Fraser, X. Wang and R. M. Kimble, *Burns*, 2006, **32**, 806–820.
6. K. R. Kirker, Y. Luo, J. H. Nielson, J. Shelby, G. D. Prestwich, *Biomaterials*, 2002, **23**, 3661–3671.
7. G. C. Gurtner, S. Werner, Y. Barrandon, M. T. Longaker, *Nature*, 2008, **453**, 314–321.
8. Y. H. Loo, Y. Wang, E. Z. Cai, C. H. Ang, A. Raju, A. Lakshmanan, *Biomaterials*, **35**, 2014, 4805–4814.
9. N. S. Gibran, S. Wiechman, W. Meyer, L. Edelman, J. Fauerbach and L. Gibbons, *J Burn Care Res*, 2013, **34**, 5–361.
10. H. Bannasch, M. Föhn, T. Unterberg, A. D. Bach, B. Wey and G. B. Stark, *Clin Plast Surg*, 2003, **30**, 573–579.
11. A. S. Klar, S. Guven, T. Biedermann, J. Luginbuhl, S. Bottcher-Haberzeth, C. Meuli-Simmen, M. Meuli, I. Martin, A. Scherberich and E. Reichmann, *Biomaterials*, 2014, **35**, 5065–5078.
12. A. S. Klar, S. Bottcher-Haberzeth, T. Biedermann, C. Schiestl, E. Reichmann and M. Meuli, *Pediatr, Surg Int*, 2014, **30**, 223–31.
13. P. L. Tremblay, V. Hudon, F. Berthod, L. Germain and F. A. A. Am, *J Transplant*, 2005, **5**, 1002–1010.
14. S. MacNeil, *Nature*, 2007, **445**, 874–880.

15. K. R. Kirker, Y. Luo, J. H. Nielson, J. Shelby and G. D. Prestwich, *Biomaterials*, 2002, **23**, 3661–3671.
16. K. L. Kim, D. K. Han, K. Park, S. H. Song, J. Y. Kim, J. M. Kim, H. Y. Ki, S. W. Yie, C. R. Roh and E. S. Jeon, *Biomaterials*, 2009, **30**, 3742–3748.
17. J. Madsen, S. P. Armes, K. Bertal, H. Lomas, S. MacNeil and A. L. Lewis, *Biomacromolecules*, 2008, **9**, 2265–2275.
18. J. Shepherd, P. Sarker, S. Rimmer, L. Swanson, S. MacNeil and I. Douglas, *Biomaterials*, 2011, **32**, 258–267.
19. B. Balakrishnan, M. Mohanty, P. R. Umashankar and A. Jayakrishnan, *Biomaterials*, 2005, **26**, 6335–6342.
20. C. He, S. W. Kim and D. S. Lee, *J Control Release*, 2008, **127**, 189–207.
21. C. T. Huynh, M. K. Nguyen and D. S. Lee, *Macromolecules*, 2011, **44**, 6629–6636.
22. L. Yu and J. D. Ding, *Chem Soc Rev*, 2008, **37**, 1473–1481.
23. D. Y. Ko, U. P. Shinde, B. Yeon and B. Jeong, *Prog Polym Sci*, 2013, **38**, 672–701.
24. H. Ma, C. He, Y. Cheng, D. Li, Y. Gong, J. Liu, H. Tian and X. Chen, *Biomaterials*, 2014, **35**, 8723–8734.
25. K. Ren, C. He, C. Xiao, G. Li and X. Chen, *Biomaterials*, 2015, **51**, 238–249.
26. G. Sun, X. Zhang, Y. Shen, R. Sebastian, L. E. Dickinson and K. Fox-Talbot, *PNAS*, 2011, **108**, 20976–20981.
27. N. Mohamad, M. C. Mohd, Amin, M. Pandey, N. Ahmad and N. F. Rajab, *Carbohydr Polym*, 2014, **114**, 312–320.
28. M. P. Ribeiro, A. Espiga, D. Silva, P. Baptista, J. Henriques, C. Ferreira, J. C. Silva, J. P. Borges, E. Pires, P. Chaves and I. J. Correia, *Wound Repair Regen*, 2009, **17**, 817–824.
29. I. A. Alsarra, *Int J Biol Macromol*, 2009, **45**, 16–21.
30. A. Ferdous, T. Akaike and A. Maruyama, *Macromolecules*, 2004, **37**, 3239–3248.
31. K. R. Kirker, Y. Luo, J. H. Nielson, J. Shelby and G. D. Prestwich, *Biomaterials*, 2002, **23**, 3661–3671.
32. J. M. Lee, J. H. Ryu, E. A. Kim, B. S. Kim and H. Lee, *Biomaterials*, **39**, 2015, 173–181.
33. T. D. Light, J. C. Jeng, A. K. Jain, K. A. Jablonski, D. E. Kim, T. M. Phillips, A. G. Rizzo and M. H. Jordan, *J Burn Care Rehabil*, 2004, **25**, 33–44.
34. L. Pescosolido, T. Piro, T. Vermonden, T. Coviello, F. Alhaique and W. E. Hennink, *Carbohydr Polym*, 2011, **86**, 208–213.
35. H. Zhao and N. D. Heindel, *Pharm Res*, 1991, **8**, 400.
36. X. G. Chen, H. J. Park, *Carbohydr Polym*, 2003, **53**, 355–359.
37. K. Murakami, H. Aoki, S. Nakamura, M. Takikawa, M. Hanzawa, S. Kishimoto, H. Hattori and Y. Tanaka, *Biomaterials*, 2010, **31**, 83–90.
38. D. K. Kweon, S. B. Song and Y. Y. Park, *Biomaterials*, 2003, **24**, 1595–1601.
39. N. T. An, D. T. Thien, N. T. Dong and P. L. Dung, *Carbohydr Polym*, 2009, **75**, 489–497.
40. A. P. Zhu, N. Fang, M. B. Chan-Park and V. Chan, *Biomaterials*, 2005, **26**, 6873–6879.
41. J. S. Boateng, K. H. Matthews, H. N. Stevens and G. M. Eccleston, *J Pharm Sci*, **2008**, **97**, 2892–2892.
42. L. Weng, X. Chen and W. Chen, *Biomacromolecules*, 2007, **8**, 1109–1115.
43. R. Mehvar, *J Control Release*, 2000, **69**, 1–25.
44. W. Lou, H. Zhang, J. Ma, D. Zhang, C. Liu, S. Wang, Z. Deng, H. Xu and J. Liu, *Carbohydr Polym*, 2012, **90**, 1024–1031.
45. E. A. Rayment, T. R. Dargaville, G. K. Shooter, G. A. George and Z. Upton, *Biomaterials*, 2008, **29**, 1785–1795.
46. B. Balakrishnan, M. Mohanty, A. C. Fernandez, P. V. Mohanan and A. Jayakrishnan, *Biomaterials*, 2006, **27**, 1355–1361.
47. J. Chang, W. Liu, B. Han, S. Peng, B. He and Z. Gu, *Wound Rep Reg*, 2013, **21**, 113–121.
48. Y. Loo, Y. C. Wong, E. Z. Cai, C. H. Ang, A. Raju, A. Lakshmanan, A. G. Koh, H. J. Zhou, T. C. Lim and S. M. Moochhala, *Biomaterials*, 2014, **35**, 4805–4814.
49. T. C. S. Cubison, S. A. Pape and N. Parkhouse, *Burns*, 2006, **32**, 992–999.
50. M. Ito, Z. X. Yang, T. Andl, C. Cui, N. Kim, S. E. Millar and G. Cotsarelis, *Nature*, 2007, **447**, 316–320.
51. M. Butcher, *Br J Nurs*, 2011, **20**, 6–51.

Graphical Abstract

In this study, the polysaccharide-based hydrogels were prepared by Schiff base reaction. Then, the hydrogels were applied to a burn wound model of rats, following by skin regeneration.

